JOURNAL OF SOLID STATE CHEMISTRY **21**, 155–160 (1977)

Structural Changes Resulting from Doping Ti_2O_3 with Sc_2O_3 or Al_2O_3

CATHERINE E. RICE AND WILLIAM R. ROBINSON*

Department of Chemistry, Purdue University, West Lafayette, Indiana 47907

Received November 22, 1976; in revised form January 21, 1977

The crystal structures of $(Ti_{1-x}Sc_x)_2O_3$, $x = 0.0038, 0.0109$, and 0.0413, and of $(Ti_{0.99}Al_{0.01})_2O_3$, have been determined from X-ray diffraction data collected from single crystals using an automated diffractometer, and have been refined to weighted residuals of 0.025–0.034. Cell constants have also been determined for $x = 0.0005$, 0.0019, and 0.0232. The compounds are rhombohedral, space group $R\bar{3}c$, and are isomorphous with α-Al_2O_3. The hexagonal cell dimensions range from $a = 5.1573(2)$ Å, $c = 13.613(1)$ Å for $(Ti_{0.9995}Sc_{0.0005})_2O_3$ to $a = 5.1659(4)$ Å, $c = 13.644(1)$ Å for $(Ti_{0.9587}Sc_{0.0413})_2O_3$, and $a = 5.1526(2)$ Å, $c = 13.609(1)$ Å for $(Ti_{0.99}Al_{0.01})_2O_3$. Sc and Al substitution cause similar increases in the short near-neighbor metal–metal distance across the shared octahedral face; for Sc doping the increase is from 2.578(1) Å in pure Ti_2O_3 to 2.597(1) Å in $(Ti_{0.9587}Sc_{0.0413})_2O_3$. By contrast, changes in the metal–metal distance across the shared octahedral edge appear to be governed by ionic size effects. The distance increases from 2.994(1) Å in Ti_2O_3 to 3.000(1) Å in $(Ti_{0.9587}Sc_{0.0413})_2O_3$ and decreases to 2.991(1) Å in $(Ti_{0.99}Al_{0.01})_2O_3$.

Ti_2O_3 undergoes a gradual semiconductor–metal transition with a concomitant distension of the crystal lattice when it is heated through the 150–350°C temperature region (*1–5*). Doping Ti_2O_3 with V_2O_3 also induces a transition to metallic behavior which is electrically (*6*, *7*) and crystallographically (*6*, *8*, *9*) similar to the transition caused by heating the pure material. In both cases the structural and electrical changes can be explained in terms of changes in metal–metal bond order which accompany the closing of a small gap between filled and empty *d* bands in the band structure of the semiconducting phase (*7*, *10*).

The properties of Ti_2O_3 doped with Sc_2O_3 are less well understood. Resistivity measurements indicate that the band gap first decreases, then increases with increasing scandium substitution (*11*). The dependence of the lattice parameters on scandium concentration appeared (*11*) to be exactly opposite to that found with vanadium doping. In order to investigate the causes for this unusual behavior, we have determined the crystal structures of $(Ti_{1-x}Sc_x)_2O_3$ for $x = 0.0038$, 0.0109, and 0.0413, and have redetermined the lattice parameters for three other scandium concentrations. The crystal structure of $(Ti_{0.99}Al_{0.01})_2O_3$ was also determined. Sc^{3+} and Al^{3+} both lack *d* electrons and so should play similar electronic roles in the Ti_2O_3 lattice, though their ionic radii differ. Thus a comparison of the structural effects of scandium and aluminum doping should help clarify whether changes in interatomic distances are due to changes in bond order or to ionic size effects.

Experimental

Samples of $(Ti_{1-x}Sc_x)_2O_3$ ($x = 0.0005$, 0.0019, 0.0038, 0.0109, 0.0232, and 0.0413) from single crystal boules were provided by Professor Honig of this department. These were the same crystals on which resistivity and lattice parameter measurements had previously been carried out (*11*). A boule of $(Ti_{0.99}Al_{0.01})_2O_3$ was grown by the Purdue

---

* Address correspondence to this author.

ISSN 0022-4596

Crystal Growth Facility by the same methods used for the Sc-doped samples. Spheres with radii ranging from 0.0160 to 0.0198 cm were ground from fragments of the boules. Film and diffractometer measurements for the crystals showed single-phase behavior and were compatible with the known space group $R\bar{3}c$ (No. 167). No significant violations of the space-group extinctions were observed.

Unit cell parameters and intensities were measured using an Enraf-Nonius CAD-4 automated diffractometer with graphite monochromated Mo$K\alpha$ radiation. The method of data collection has been described previously (*9*). Hexagonal cell parameters and their ESDs, shown in Table I, were calculated by least-squares refinement of the observed 2θ values for 50 to 60 reflections per crystal, $80° < 2\theta < 100°$, using the program LCR-2 (*12*) with $\lambda(\mathrm{Mo}K\alpha_1) = 0.70926$ Å. The intensities of all reflections in a hemisphere of reciprocal space with $6° < 2\theta < 66°$ were collected for all samples whose structures were determined. After applying Lorentz polarization and spherical absorption corrections (μR ranged from 0.61 to 0.75), equivalent reflections were averaged to give 126 independent reflections for each intensity data set. Reflections with $I < \sigma(I)$ were set equal to $\frac{1}{2}\sigma(I)$ and included in the refinement.

Least-squares refinements using both isotropic and anisotropic temperature factors were carried out for each set of intensity data using the RFINE2 program of Finger (*13*). The initial atomic parameters in the space group $R\bar{3}c$ were those of Robinson (*14*) for Ti_2O_3, transformed from rhombohedral to hexagonal coordinates. The program minimized $\sum w(F_o - F_c)^2$ using the scattering factors for Ti^{3+}, Sc^{3+}, Al^{3+}, and O^{0} (*15*) corrected for real and imaginary anomalous dispersion (*16*), weights based on average standard deviations determined from counting statistics ($w = 1/\sigma^2(F) = 4F_0{}^2/\sigma^2(F_0{}^2)$), and an extinction correction of the form $F^2_{\mathrm{corr}} = F_0{}^2(1 + sI_0{}^2)$. No reflections were rejected from the refinements. Final weighted R values varied from 0.025 to 0.034. Values of the standard deviation of an observation of unit weight are listed in Table II as S. The final atom parameters in Table II were used with the variance–covariance matrices to calculate the interatomic distances and angles and their ESDs listed in Table III. Structure factor amplitudes are reported in Table IV.

TABLE I

UNIT CELL PARAMETERS FOR $(Ti_{1-x}Sc_x)_2O_3$ AND $(Ti_{0.99}Al_{0.01})_2O_3$ WITH STANDARD DEVIATIONS IN PARENTHESES

Dopant concentration	a_{hex} (Å)	c_{hex} (Å)
Pure Ti_2O_3[a]	5.1580(4)	13.611(1)
0.05 at% of Sc	5.1573(2)	13.613(1)
0.19 at% of Sc	5.1586(3)	13.611(1)
0.38 at% of Sc	5.1589(2)	13.616(1)
1.09 at% of Sc	5.1598(1)	13.625(1)
2.32 at% of Sc	5.1618(2)	13.632(2)
4.13 at% of Sc	5.1659(4)	13.644(1)
1 at% of Al	5.1526(2)	13.609(1)

[a] Ref. (*5*).

Results and Discussion

All crystals studied were found to be isomorphous with α-Al_2O_3. The structures consist of approximate hexagonally closest-packed oxide layers with metal ions occupying two-thirds of the octahedral interstices (Fig. 1). A given metal ion, $M(1)$, has one near metal neighbor along the c axis with which it shares a triangular face of its coordination octahedron ($M(2)$ in Fig. 1), and three near metal neighbors in the a–b plane which share edges of the octahedron ($M(3)$ in Fig. 1).

The effects of scandium and aluminum doping on the Ti_2O_3 lattice parameters are shown in Table I. Cell constants for Ti_2O_3 (*5*) are also included for comparison. Many unit cell determinations (*17*) and three refined crystal structures from single crystal data (*5*, *14*, *18*) are available for Ti_2O_3. This set was chosen since it was determined on the same instrument under the same conditions as the other data reported and thus comparisons of the small changes observed should not be effected by possible systematic errors between equipment or by differences in conditions.

Doping with Sc^{3+} or Al^{3+} causes only

TABLE II

CRYSTALLOGRAPHIC DATA FOR $(Ti_{1-x}Sc_x)_2O_3$ AND $(Ti_{0.99}Al_{0.01})_2O_3$ WITH STANDARD DEVIATIONS IN PARENTHESES

Parameter	0.38 at% of Sc	1.09 at% of Sc	4.13 at% of Sc	1 at% of Al
M z	0.34470(5)	0.34486(5)	0.34517(4)	0.34487(4)
β_{11}[a]	30(4)	28(4)	34(3)	32(4)
β_{33}[a]	3.6(6)	1.7(6)	5.5(4)	4.2(4)
Ox x	0.3130(4)	0.3130(4)	0.3123(3)	0.3130(3)
β_{11}[a]	33(8)	28(7)	35(6)	36(6)
β_{22}[a]	44(11)	36(10)	52(8)	41(8)
β_{33}[a]	3.3(12)	1.5(10)	5.3(8)	3.1(8)
β_{13}[a]	0.8(12)	1.0(11)	1.7(10)	2.2(10)
R	0.024	0.026	0.018	0.019
R_{wt}	0.034	0.032	0.025	0.026
s[b]	5.2(5)	6.0(5)	3.7(3)	3.9(3)
B_M	0.25(3)	0.19(3)	0.32(2)	0.29(2)
B_{Ox}	0.28(4)	0.20(4)	0.35(3)	0.34(3)
S	1.00	1.00	1.00	1.07

[a] Times 10^4. For M, $\beta_{11} = \beta_{22}$, $\beta_{12} = \frac{1}{2}\beta_{11}$, and $\beta_{23} = \beta_{13} = 0$. For Ox, $\beta_{12} = \frac{1}{2}\beta_{22}$ and $\beta_{23} = 2\beta_{13}$. The form of the anisotropic temperature factor T is $T = \exp(-\sum_i \sum_j h_i h_j \beta_{ij})$.

[b] Times 10^5.

TABLE III

INTERATOMIC DISTANCES (Å) AND BOND ANGLES (DEGREES) FOR $(Ti_{1-x}Sc_x)_2O_3$ AND $(Ti_{0.99}Al_{0.01})_2O_3$, WITH STANDARD DEVIATIONS IN PARENTHESES

	Pure Ti_2O_3[a]	0.38 at% of Sc	1.09 at% of Sc	4.13 at% of Sc	1 at% of Al
		Distances			
$M(1)$–$M(2)$	2.578(2)	2.579(1)	2.585(1)	2.597(1)	2.582(1)
$M(1)$–$M(3)$	2.994(1)	2.995(1)	2.996(1)	3.000(1)	2.991(1)
$M(1)$–O(1)	2.066(2)	2.066(2)	2.068(2)	2.071(1)	2.066(1)
$M(1)$–O(5)	2.027(1)	2.027(1)	2.026(1)	2.029(1)	2.024(1)
O(1)–O(2)	2.796(4)	2.797(4)	2.797(3)	2.794(3)	2.789(1)
O(1)–O(4)	2.791(1)	2.791(1)	2.792(1)	2.794(1)	2.793(2)
O(1)–O(5)	2.880(1)	2.881(1)	2.882(1)	2.887(1)	2.878(1)
O(4)–O(5)	3.073(2)	3.074(2)	3.074(2)	3.081(2)	3.070(1)
		Angles			
O(1)–$M(1)$–O(2)	85.20(7)	85.17(6)	85.09(6)	84.85(4)	85.07(4)
O(1)–$M(1)$–O(4)	85.96(2)	85.97(2)	85.98(2)	85.94(1)	85.99(1)
O(1)–$M(1)$–O(5)	89.42(5)	89.45(5)	89.46(4)	89.53(4)	89.47(3)
O(1)–$M(1)$–O(6)	170.01(8)	169.99(7)	169.90(7)	169.60(5)	169.88(5)
O(4)–$M(1)$–O(5)	98.60(3)	98.60(3)	98.65(3)	98.81(2)	98.65(2)
$M(1)$–O(1)–$M(2)$	77.18(9)	77.23(8)	77.34(7)	77.66(6)	77.37(5)
$M(1)$–O(2)–$M(3)$	94.04(2)	94.03(2)	94.02(2)	94.06(1)	94.01(1)
$M(2)$–O(2)–O(3)	132.33(5)	132.34(4)	132.33(4)	132.37(3)	132.34(3)

[a] Ref. (5).

TABLE IV

VALUES OF 10 F_{obs} AND 10 F_{calc}.

			.38% Sc		1.09% Sc		4.13% Sc		1% Al	
H	K	L	FOBS	FCALC	FOBS	FCALC	FOBS	FCALC	FOBS	FCALC
0	0	6	657	707	669	701	646	699	636	682
0	0	12	1100	1078	1117	1075	1057	1067	1084	1095
0	0	18	46	57	73	73	71	91	53	74
0	1	2	787	809	764	798	813	817	787	753
0	1	8	144	126	157	139	169	160	137	135
0	1	14	436	434	469	460	453	455	423	426
0	1	20	583	587	610	633	578	575	570	546
0	2	4	1121	1141	1093	1127	1187	1191	1135	1137
0	2	10	987	971	1021	975	982	987	965	983
0	2	16	849	838	888	862	825	819	836	816
0	3	6	657	658	651	654	654	654	633	645
0	3	12	896	883	920	887	870	859	867	875
0	3	18	35	35	48	50	58	65	62	50
0	4	2	550	557	565	555	559	557	539	546
0	4	8	161	164	172	174	187	186	163	164
0	4	14	288	286	302	307	296	302	275	270
0	5	4	731	734	736	735	743	749	709	723
0	5	10	656	667	673	677	655	660	635	636
0	6	6	478	497	493	496	485	490	468	460
1	0	4	1084	1143	1055	1129	1151	1189	1095	1086
1	0	10	1135	1122	1138	1121	1150	1154	1120	1146
1	0	16	830	815	860	838	811	792	802	792
1	1	0	1147	1205	1111	1182	1190	1250	1144	1146
1	1	3	775	739	763	735	796	750	764	727
1	1	6	1439	1426	1420	1399	1492	1481	1437	1438
1	1	9	455	454	469	460	452	451	436	449
1	1	12	510	509	525	511	471	473	485	480
1	1	15	268	278	285	290	262	267	258	267
1	1	18	347	357	359	364	307	301	340	318
1	2	2	535	533	534	529	535	527	522	523
1	2	5	122	118	126	118	114	120	118	115
1	2	8	56	35	50	46	72	63	60	43
1	2	11	69	75	74	76	75	74	67	71
1	2	14	428	431	453	456	442	448	411	418
1	2	17	47	52	52	54	46	49	46	48
1	3	1	80	79	80	80	78	83	76	77
1	3	4	752	753	754	751	778	765	736	751
1	3	7	68	66	75	67	77	70	65	64
1	3	10	918	908	920	915	932	923	897	912
1	3	13	65	50	55	52	55	52	58	48
1	3	16	683	691	705	715	662	662	663	647
1	4	3	282	282	289	286	282	278	273	272
1	4	6	950	934	949	929	959	941	928	938
1	4	9	232	238	239	245	230	231	226	251
1	4	12	398	410	406	413	380	379	377	371
1	5	2	266	270	270	269	257	262	255	251
1	5	5	101	116	115	119	118	117	107	109
1	5	8	36	13	38	8	41	6	25	7
1	5	11	92	101	95	105	94	99	93	93
1	6	1	59	64	54	65	65	67	56	59
2	0	2	537	533	524	528	520	523	518	521
2	0	8	76	10	31	3	39	21	36	3
2	0	14	464	478	493	503	503	495	465	465
2	1	1	151	141	152	141	155	145	147	139
2	1	4	1007	991	986	983	1022	1025	983	1000
2	1	7	101	105	102	107	100	109	99	103
2	1	10	961	940	966	945	956	955	928	950
2	1	13	73	69	66	72	66	71	64	67
2	1	16	794	789	820	814	767	766	769	759
2	2	0	990	967	974	954	1005	991	976	978
2	2	3	397	406	411	408	404	404	392	398
2	2	6	1141	1111	1126	1099	1159	1133	1127	1141
2	2	9	307	307	314	313	299	301	292	297
2	2	12	440	447	450	450	409	415	421	413
2	2	15	218	227	226	237	210	216	208	213
2	3	2	315	311	308	310	299	301	299	297
2	3	5	83	84	87	85	88	85	78	80
2	3	8	32	31	55	24	44	10	40	22
2	3	11	62	67	64	69	64	66	64	63
2	3	14	404	416	418	439	413	426	385	391
2	4	1	105	107	107	109	108	110	103	101
2	4	4	612	623	621	626	627	628	605	603
2	4	7	97	99	102	102	101	103	95	94
2	4	10	713	718	715	729	714	719	693	688
2	5	3	177	180	177	184	172	174	169	167
2	5	6	746	753	756	756	750	745	734	719
3	0	0	1590	1558	1549	1523	1669	1638	1603	1612
3	0	6	656	658	638	654	652	653	627	645
3	0	12	899	883	888	888	884	860	861	875
3	0	18	35	35	37	50	56	66	73	51
3	1	2	541	545	548	541	547	543	525	533
3	1	5	68	70	68	70	68	71	64	66
3	1	8	134	121	136	131	148	144	123	123
3	1	11	41	50	46	51	43	49	41	46
3	1	14	337	336	354	359	348	352	325	320
3	1	17	38	38	38	39	32	34	28	33
3	2	1	89	91	93	92	90	93	85	88
3	2	4	807	795	800	794	816	814	786	794
3	2	7	77	79	84	81	81	81	77	76
3	2	10	735	730	729	739	730	728	707	709
3	2	13	61	63	66	66	61	63	58	60
3	3	0	1110	1063	1094	1053	1110	1087	1087	1088
3	3	3	35	4	15	4	22	3	27	4
3	3	6	521	533	533	531	523	526	508	503
3	3	9	27	3	23	4	22	2	35	3
3	3	12	686	686	672	696	653	653	656	645
3	4	2	403	413	401	415	395	408	392	385
3	4	5	22	29	24	29	33	28	28	25
3	4	8	141	143	146	153	153	159	138	137
4	0	4	655	653	656	653	659	660	635	645
4	0	10	913	905	891	912	934	918	891	906
4	0	16	624	641	622	664	612	611	612	591
4	1	0	832	820	841	812	848	832	818	817
4	1	3	286	282	290	286	256	278	271	272
4	1	6	973	934	951	929	950	941	925	938
4	1	9	234	239	241	245	231	232	225	227
4	1	12	405	410	401	413	375	379	382	371
4	2	2	334	342	342	341	328	335	322	322
4	2	5	96	101	96	102	99	101	92	94
4	2	8	50	43	65	49	69	60	45	44
4	2	11	72	86	79	87	78	83	73	77
4	3	1	25	31	40	31	45	32	34	28
4	3	4	452	460	457	463	451	458	438	430
4	3	7	32	30	41	31	35	32	36	28
5	0	2	263	262	262	262	252	252	250	248
5	0	8	38	42	46	35	51	22	41	31
5	1	1	120	122	122	124	125	124	117	115
5	1	4	656	651	650	654	658	658	623	629
5	1	7	110	114	111	117	117	116	105	107
5	1	10	650	653	647	664	644	649	618	616
5	2	0	652	661	664	658	663	664	637	628
5	2	3	177	180	180	185	172	174	169	167
5	2	6	763	753	756	756	744	746	730	719
6	0	0	961	948	972	943	980	960	954	944
6	0	6	487	496	487	496	481	489	472	459
6	1	2	328	342	336	344	330	336	317	313

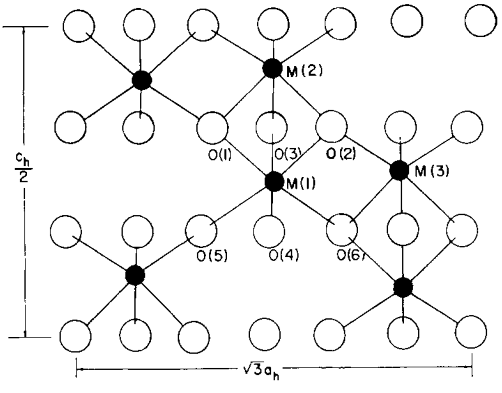

FIG. 1. A projection of the corundum structure on a plane perpendicular to the [110] axis.

small changes in the c axis of Ti_2O_3, with scandium showing the greatest effect: c increases slightly upon addition of scandium and may decrease upon addition of aluminum. The radii of the ions vary in the order Sc^{3+} (0.730 Å) > Ti^{3+} (0.67 Å) $\gg$ Al^{3+} (0.530 Å) (*19*). If the structural changes were governed solely by ionic size effects, one would expect a greater decrease in the c axis with Al doping and an increase with Sc doping which is smaller than that observed. On the other hand, the changes in the a axis with doping are more in keeping with ionic size changes. Adding scandium causes a to increase, while added Al causes a to decrease.

The cell constants we have measured for scandium-doped Ti_2O_3 are quite different from those reported by Chandrashekhar *et al.* (*11*) using the same samples. These authors reported a decrease in the c axis and almost no change in the a axis with increasing Sc content. We believe that the discrepancies between the two sets of data arise from the use by the previous authors of limited data sets (about six reflections with $20° < 2\theta < 70°$) and refinement procedures which included no corrections for absorption, sample eccentricity, or calibration error (*20*).

The effects of Sc and Al doping on the Ti_2O_3 structure are apparent mainly in the metal–metal distances, whose behavior is shown in Table III and Fig. 2. The data for V-doped Ti_2O_3 (*9*) are included in the figure for comparison. The distance between metal ions sharing a face of their coordination polyhedra, $M(1)$–$M(2)$, increases from 2.578(2) Å in Ti_2O_3 to 2.597(1) Å in $(Ti_{0.9587}Sc_{0.0413})_2O_3$, and to 2.582(1) Å in $(Ti_{0.99}Al_{0.01})_2O_3$. The increase in the $M(1)$–$M(2)$ distance caused by

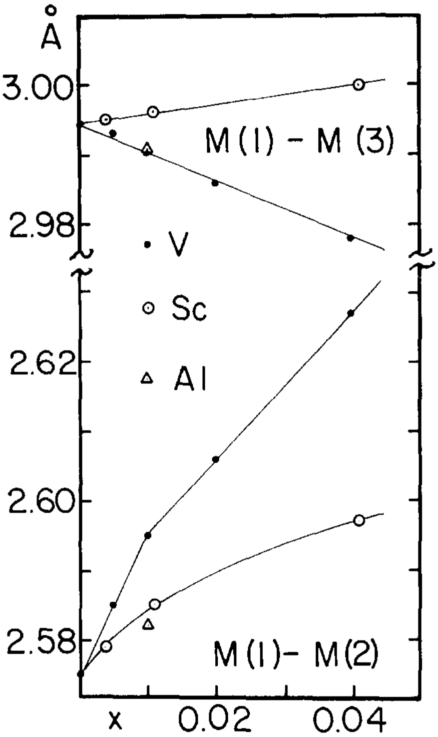

FIG. 2. Variation of metal–metal distances in $(Ti_{1-x}M_x)_2O_3$.

1% of Al substitution is almost identical to the change produced by 1% of Sc. The increase in both cases is about half that caused by the same concentration of vanadium. The metal–metal distance across the shared edge, $M(1)$–$M(3)$, increases from 2.994(1) Å in Ti_2O_3 to 3.000(1) Å in $(Ti_{0.9587}Sc_{0.0413})_2O_3$ while it decreases to 2.991(1) Å in $(Ti_{0.99}Al_{0.01})_2O_3$. The changes in the $M(1)$–$M(3)$ distance with Al and Sc doping are close to those expected due to changes in effective ionic radius, though the changes caused by V-doping are greater than one would predict on this basis alone.

Changes in metal–oxygen and oxygen–oxygen distances with Sc or Al doping are small, with a maximum change of 0.005 Å in the metal–oxygen distances. The entire structural change in both cases can be explained satisfactorily as the result of changes in the metal–metal distances coupled with reorganization of the structure in order to maintain approximately constant metal–oxygen distances.

The effects of doping Ti_2O_3 with Sc or Al can be understood in terms of the band-crossing scheme proposed (*10*) to account for the electrical behavior of pure Ti_2O_3. In this model the valence band, a band of a_1 symmetry, is formed by the bonding interaction between d_{z^2} orbitals of c axis neighbor metal ions, $M(1)$ and $M(2)$. This band is completely filled at 0°K. At low temperatures, the valence band is separated by a small gap from the conduction band, of e symmetry, which is formed by overlap of d orbitals of near-metal neighbors in the a–b plane ($M(1)$ and $M(3)$). The semiconductor–metal transitions caused in Ti_2O_3 by heating or by doping with vanadium involve removal of electrons from the a_1 band with a decrease in the $M(1)$–$M(2)$ bond order and a concomitant increase in the $M(1)$–$M(2)$ distance. This increase of the $M(1)$–$M(2)$ distance destabilizes the a_1 band so that it rises in energy and eventually overlaps the e band, resulting in metallic behavior. Single-crystal X-ray studies have confirmed that substantial increases in the $M(1)$–$M(2)$ distance accompany the electrical transitions in both pure and V-doped Ti_2O_3 (*4*, *5*, *9*). The detailed mechanisms for these transitions using this model have been discussed elsewhere (*2*, *7*, *10*).

Since neither Sc^{3+} nor Al^{3+} possesses d electrons, these ions are not likely to participate in metal–metal bonding in the Ti_2O_3 host lattice. Thus the addition of each Sc^{3+} or Al^{3+} ion should disrupt one $M(1)$–$M(2)$ bond, increasing the average $M(1)$–$M(2)$ distance and generally dilating the structure in the c direction. As the $M(1)$–$M(2)$ distance increases, the a_1 band should then rise in energy and cause the band gap to decrease (*10*, *21*, *22*). This would explain why the activation energy for conduction, ε_a, initially decreases as Sc is added to Ti_2O_3. The eventual increase in ε_a with greater Sc substitution can be related to the increase in the $M(1)$–$M(3)$ distance, which increases more slowly with increasing dopant concentration than does the $M(1)$–$M(2)$ distance. The e band in Ti_2O_3 formed by overlap between orbitals of $M(1)$ and $M(3)$ has been shown to be narrow (*21*, *22*), probably because the $M(1)$–$M(3)$ distance is already rather long for effective metal–metal overlap. The increase in this distance caused by the greater size of the Sc^{3+} ion and the presence of the dopant ion should narrow the *e* band even more. This, though the *M*(1)–*M*(2) increase should cause the a_1 and *e* band centers to move together, band narrowing may widen the band gap when the dopant concentration is sufficiently large.

The structural effects of Sc substitution in Ti_2O_3 are thus compatible with the Ti_2O_3 band structure and with the observed nonmonotonic dependence of ε_a on dopant concentration (*11*). The structure of $(Ti_{0.99}Al_{0.01})_2O_3$ tends to confirm our interpretation. Since Sc and Al substitution have similar effects on the *M*(1)–*M*(2) distance, this change must be due to a change in bond order. The changes in the *M*(1)–*M*(3) distance with doping, however, are apparently related to ionic size effects. Resistivity measurements on a series of aluminum doped Ti_2O_3 samples are in progress to check the variation of ε_a with the *M*(1)–*M*(3) distance.

Acknowledgments

We would like to thank Professor J. M. Honig for providing samples and for enlightening discussions, George Yuochonas for the growth of crystals used in this work, and the Stauffer Chemical Company for award of a fellowship to C.E.R. This work was supported by the National Science Foundation NSF-MRL Program DMR-7203018-A04.

References

1. F. J. Morin, *Phys. Rev. Lett.* **3**, 34 (1959).

2. J. M. Honig and T. B. Reed, *Phys. Rev.* **174**, 1020 (1968).

3. C. N. R. Rao, R. E. Loehman, and J. M. Honig, *Phys. Lett.* **27A**, 271 (1968).

4. C. E. Rice and W. R. Robinson, *Mat. Res. Bull.* **11**, 1355 (1976).

5. C. E. Rice and W. R. Robinson, *Acta Crystallogr.* in press.

6. T. Kawakubo, T. Yanagi, and S. Nomura, *J. Phys. Soc. Japan* **15**, 2102 (1960).

7. G. V. Chandrashekhar, Q. Won Choi, J. Moyo, and J. M. Honig, *Mat. Res. Bull.* **5**, 999 (1970).

8. R. E. Loehman, C. N. R. Rao, and J. M. Honig, *J. Phys. Chem.* **73**, 1781 (1969).

9. C. E. Rice and W. R. Robinson, *J. Solid State Chem.* **21**, 145 (1977).

10. L. L. van Zandt, J. M. Honig, and J. B. Goodenough, *J. Appl. Phys.* **39**, 594 (1968).

11. G. V. Chandrashekhar, L. L. van Zandt, J. M. Honig, and A. Jayaraman, *Phys. Rev. B* **10**, 5063 (1974).

12. D. E. Williams "LCR-2, a Fortran Lattice Constant Refinement Program," IS-1052, Iowa State University, Ames, Iowa, 1964.

13. L. W. Finger, "RFINE2, a Fortran IV Program for Structure Factor Calculation and Least-Squares Refinement of Crystal Structures," Geophysical Laboratory, Washington, D.C., 1972.

14. W. R. Robinson, *J. Solid State Chem.* **9**, 255 (1974).

15. D. T. Cromer and J. T. Waber, *Acta Crystallogr.* **18**, 104 (1965).

16. D. T. Cromer, *Acta Crystallogr.* **18**, 17 (1965).

17. "Landolt-Börnstein, New Series, Group III," (K. H. Hellwege and A. M. Hellwege, Eds.), Vol. 7b, p. 299. Springer-Verlag, Berlin, 1975.

18. R. E. Newnham and Y. M. De Haan, *Z. Kristallogr.* **117**, 235 (1962).

19. R. D. Shannon and C. T. Prewitt, *Acta Crystallogr.* **B 25**, 925 (1969).

20. J. M. Honig, personal communication.

21. T. C. Chi and R. J. Sladek, *Phys. Rev. B* **7**, 5080 (1973).

22. H. L. Barros, G. V. Chandrashekhar, T. C. Chi, J. M. Honig, and R. J. Sladek, *Phys. Rev. B* **7**, 5147 (1973).